# Assessment of Ischemia-Induced Microvascular Remodeling Using Contrast-Enhanced Ultrasound Vascular Anatomic Mapping

Marco Pascotto, MD, Howard Leong-Poi, MD, Beat Kaufmann, MD, Achim Allrogen, MD, Dimitrios Charalampidis, PhD, Edmund K. Kerut, MD, Sanjiv Kaul, MD, FASE, and Jonathan R. Lindner, MD, FASE, *Charlottesville, Virginia; Portland, Oregon; and New Orleans, Louisiana*

**Our aim was to apply novel contrast-enhanced ultrasound (CEU) techniques to characterize remodeling in different vascular compartments during ischemia-mediated angiogenesis. Hind limb ischemia was produced by ligation of an external iliac artery in 60 rats, half of which were treated with intramuscular fibroblast growth factor (FGF)-2 (5 μg). The proximal adductor muscles of the ischemic and control hind limb were studied immediately after ligation and at days 4, 7, or 14. Low-power maximum intensity projection imaging was performed to assess large intramuscular vessels to the fourth branch order. CEU data were analyzed to measure capillary perfusion and functional noncapillary microvascular blood volume. Resting capillary perfusion was reduced by 30% after arterial ligation and recovered earlier in FGF-2–treated versus nontreated rats (day 4 vs. 14). Changes in perfusion were temporally related to expansion of noncapillary microvascular blood volume on CEU, which was associated with an arteriogenic response on histology. Expansion of and organization (fractal distribution) of large collateral vessels occurred gradually over 2 weeks and was slightly more rapid with FGF-2 treatment. We conclude that CEU can separately assess collateral development, more distal arteriogenesis, and secondary changes in capillary perfusion that occur differentially with ischemia and growth factor therapy.** (J Am Soc Echocardiogr 2007; 20:1100-1108.)

Vascular remodeling in response to chronic occlusive arterial disease occurs through a continuum that involves the development and enlargement of large collateral vessels, arteriogenesis in more distal vessels, and formation of new capillaries.[1,2] The ability to fully characterize the temporal and spatial pattern of these different processes is important for understanding adaptive responses to ischemia and how they can be manipulated to improve tissue perfusion. Morphometry of medium to large vessels has traditionally been assessed by angiography or postmortem techniques, such as vascular casting, histology, and high-resolution micro-computed tomography.[3] Alternatively, the total impact of vascular remodeling can be evaluated by noninvasive imaging of tissue perfusion.[4,5] However, tools are lacking to characterize the functional changes to ischemia that occur over time along the entire vascular network, from large branch vessels to the capillary level.

Contrast-enhanced ultrasound (CEU) is a noninvasive imaging technique capable of assessing microvascular blood flow, blood volume, and velocity.[6] By taking advantage of the normal hierarchic relationship between vessel dimension and flow velocity,[7] it is possible to differentiate changes in blood volume and blood flow that occur in the capillary bed from those in the noncapillary microvessels (NCM) with CEU. This strategy was recently used to evaluate insulin-mediated capillary responses and shunting from non-nutritive to nutritive vascular pathways in limb skeletal muscle.[8,9] The ability to characterize the architecture of large microvessels has also re-

From the Cardiovascular Division, University of Virginia, Charlottesville, Virginia; Division of Cardiovascular Medicine, Oregon Health and Sciences University, Portland, Oregon; Department of Electrical Engineering, University of New Orleans, New Orleans, Louisiana; and Cardiovascular Division, Louisiana State University, New Orleans, Louisiana.

Drs. Pascotto and Leong-Poi contributed equally to this study.

Supported by grants (R01-HL-074443, R01-HL-078610 and R01-DK-063508) to Dr. Lindner and (R01-EB-002069) to Dr. Kaul from the National Institutes of Health, Bethesda, Maryland. Dr. Leong-Poi was supported by a Research Fellowship Award from the Canadian Institutes of Health Research and the Heart and Stroke Foundation of Canada, Ottawa, Canada. Dr. Kaufmann is supported by research grants from the Swiss National Science Foundation.

Reprint requests: Jonathan R. Lindner, MD, Division of Cardiovascular Medicine, Oregon Health and Sciences University, 3181 SW Sam Jackson Park Road, UHN-62, Portland, OR 97239 (E-mail: *lindnerj@ohsu.edu*).

0894-7317/$32.00



doi:10.1016/j.echo.2007.02.016

cently become possible by high-frequency contrast-enhanced maximum-intensity projection (MIP) imaging. The aim of this study was to apply these diverse CEU techniques to characterize vascular adaptations in a model of limb ischemia, with and without growth factor therapy. MIP imaging was used to temporally assess functionality of large collateral circuits, whereas microvascular perfusion data were modeled to evaluate proliferation of distal NCM that participate in flow distribution and network resistance, and the subsequent changes in skeletal muscle nutritive perfusion at the capillary level.

## MATERIALS AND METHODS

### Animal Preparation and Study Protocol

The study protocol was approved by the institutional Animal Care and Use Committee. Proximal hind limb ischemia was produced in 60 male Sprague-Dawley rats. Animals were anesthetized with an intraperitoneal injection of ketamine hydrochloride (10 mg/kg$^{-1}$), xylazine (8 mg/kg$^{-1}$), and atropine (0.02 mg/kg$^{-1}$). With an aseptic technique, the left external iliac artery and small proximal branches were ligated. In 30 animals, the proximal hind limb adductor muscles (adductor magnus and semimembranosus) distal to the ligature were treated with fibroblast growth factor (FGF)-2 by intramuscular injection of heparin-agarose alginate microcapsules containing 5 μg of FGF-2 to produce sustained growth factor release.[10] The ischemic and contralateral control limb were imaged immediately after arterial ligation in all animals, and at day 4, 7, or 14. For each imaging study, MIP imaging was performed at rest and CEU perfusion imaging was performed at rest and during contractile exercise-induced hyperemia produced by electrostimulation of the adductor muscle group at 2 Hz using 5 mA square wave pulses. On completion of imaging, skeletal muscle from both limbs was obtained for immunohistochemistry.

### Assessment of Capillary Perfusion and Noncapillary Microvascular Blood Volume

CEU of the proximal hind limb adductor muscles half distance to the knee was performed in the transaxial plane with ultraharmonic imaging (Sonos 5500, Philips Ultrasound, Andover, Mass) at a transmission frequency of 1.3 MHz and a mechanical index of 1.0. The femur-muscle orientation was used to ensure a consistent imaging plane. The acoustic focus was placed at the level of the adductor muscles. The elevational plane dimension at the focal depth was 4 mm according to needle hydrophone measurements (PVDF-Z44, Specialty Engineering Associates, Sunnyvale, Calif). The dynamic range was set at maximal, and gain settings were optimized and held constant. For contrast enhancement, lipid-shelled microbubbles were prepared by sonication of a decafluorobutane gas-saturated aqueous solution of distearoylphosphatidylcholine and PEG-stearate, and their concentration was determined by electrozone sensing (Multisizer IIe, Beckman-Coulter, Fullerton, Calif). Microbubbles were administered as a continuous intravenous infusion at $1 \times 10^7$ min$^{-1}$. Images were first acquired at 20 Hz and then during progressive prolongation of the pulsing interval from 1 to 20 seconds.

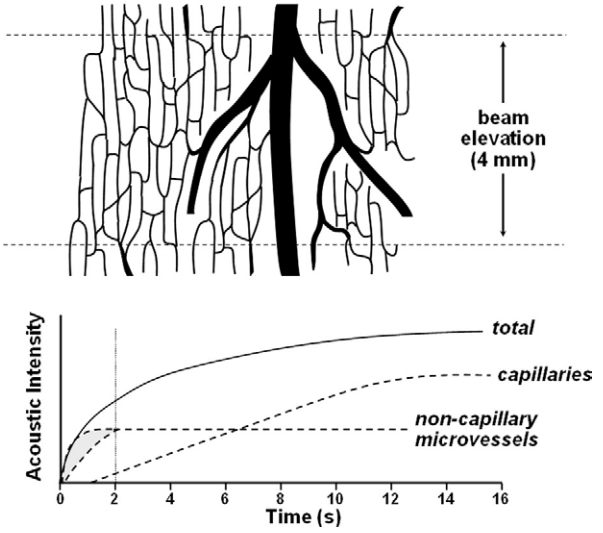


**Figure 1** Schematic illustration for assessing capillary perfusion and NCM blood volume. With transaxial-plane imaging, the largest microvessels with the fastest flow velocity are oriented along the elevational axis. Curve-fitted, background-subtracted pulsing interval versus acoustic intensity data provided information on microvascular blood velocity (rate constant β) and volume (plateau intensity or A value) from the total microcirculation within the imaging sector. Subsequent analysis using a pulsing interval of 2 seconds as background eliminated information from NCM that possess variable velocities greater than 2 mm/s. This second analysis yielded information on the capillary compartment alone, although elimination of a small portion of the capillary signal would also be expected. An index of NCM blood volume was derived by the difference between the plateau intensities (A values) for total microvascular and capillary blood volume.

Data were determined from regions of interest placed on the adductor muscles containing a tissue volume of 80 to 120 mm$^3$. Figure 1 schematically depicts the method for distinguishing capillary from NCM. Several averaged frames acquired at 20 Hz were digitally subtracted from averaged frames at each pulsing interval to eliminate signal from both tissue and large intramuscular vessels with a flow velocity sufficiently rapid to completely replenish the imaging sector between pulses (≥8 cm/s based on beam elevational dimension).[8] The resulting pulsing-interval versus acoustic intensity data from the muscle, reflecting the total microvascular compartment was fit to the function:

$$y = A(1\text{-e-}\beta t)1$$

where $y$ is acoustic intensity at the pulsing interval $t$, $A$ is the plateau acoustic intensity that reflects relative micro-

vascular blood volume, β is the rate constant that reflects microvascular blood velocity, and the product of *A* and β is flow.[6] Values were recalculated using averaged frames at a pulsing interval of 2 seconds as background to eliminate vessels with a transaxial plane velocity of greater than 2 mm/s. Under resting conditions, this recalculation would be expected to yield information at the capillary compartment alone and was used to determine capillary blood flow and volume. The relative NCM blood volume was determined by the difference of the calculated *A* values.

### Maximum Intensity Projection Imaging

For anatomic mapping of medium to large intramuscular vessels, CEU was performed by MIP imaging (Aplio, Toshiba Medical Imaging, Tustin, Calif), which displays the intensity of any given pixel as a persistence of the maximal intensity achieved. Phase-inversion harmonic imaging in the sagittal plane was performed with a linear-array transducer at a frequency of 5.5 MHz, a frame rate of 15 Hz, and a dynamic range of 40 dB. Microbubbles ($1 \times 10^7$) were administered as a rapid intravenous bolus injection. After contrast appearance in the limb, microbubbles were destroyed by a high-power three-frame sequence at a mechanical index of 1.4. MIP image sets were then acquired over 2 seconds using nondestructive low-power imaging at a mechanical index of 0.2. Imaging was performed in three adjacent longitudinal planes. A measure of total vascular density was determined in a region of interest placed over the entire muscle by digitally subtracting the final frame of the 2-second acquisition from averaged precontrast frames. Flow velocity in the distal branch order vessels was measured by frame-by-frame tracking the leading edge of contrast enhancement with calibrated video calipers. Fractal dimension of vascular distribution in tissue was calculated on the final MIP imaging frame using the variation method.[11] This mathematic algorithm, described in detail in the Appendix, provides an index of scale-independent roughness of contrast enhancement that was used to assess ordered distribution of actively perfused vessels in the spatial domain.

### Immunohistology

Staining was performed on fixed, paraffin-embedded proximal hind limb adductor muscle sectioned in the transaxial plane. For endothelial cell staining, mouse anti-rat CD31 monoclonal antibody (MAB1393, Chemicon, Temecula, Calif) was used with an fluorescein isothiocyanate-labeled secondary antibody (Santa Cruz Biotechnology, Santa Cruz, Calif). For smooth muscle α-actin staining, a mouse primary monoclonal antibody (1A4, Sigma, St. Louis, Mo) was used with an ALEXA-555–labeled secondary antibody (Molecular Probes, Invitrogen, Carlsbad, Calif). Coverslipping was performed with the mounting medium containing DAPI (Vector Labs, Burlingame, CA). Fluorescent microscopy was performed with excitation filters of 320 to 380 nm, 460 to 500 nm, and 530 to 560 nm. Capillary density per myocyte was determined by vessels that stained only for CD31 in transverse muscle sections. The density and two-dimensional area of NCM was determined by the number and cumulative area for vessels that stained positive for smooth muscle α-actin, expressed as a percentage of the total muscle area. The cumulative area calculations were based on the smallest dimension through the vessel centroid.

### Statistical Methods

Data were analyzed with RS/1 (version 6.0.1, Domain Manufacturing, Corp., Burlington, Mass). Data are expressed as mean (±1 standard deviation). Comparisons between single continuous variables were made using paired or unpaired Student *t* test (two-tailed). Comparisons between multiple stages or between groups were made with one-way analysis of variance and by Bonferroni correction for multiple comparisons. Differences were considered significant at a *P* value less than .05.

## RESULTS

### Skeletal Muscle Capillary Blood Flow

Immediately after arterial ligation, resting skeletal muscle capillary blood flow in the ischemic limb measured by CEU was reduced by approximately 30% compared with that in the contralateral control limb. Reduction in blood flow was associated with an average 20% decrease in capillary blood velocity and a 12% reduction in capillary blood volume. Changes in capillary blood flow in the ischemic limb over the ensuing 2 weeks differed according to treatment group (Figure 2A). Recovery in resting skeletal muscle capillary perfusion occurred earlier in animals treated with FGF-2 compared with untreated animals (day 4 vs. day 14). Parametric assessment of perfusion indicated that improvement in capillary blood flow was attributable to favorable changes in capillary blood velocity more than capillary blood volume (Table). Immunohistology for CD31-positive but smooth muscle α-actin–negative vessels did not demonstrate any significant change in anatomic capillary density in the adductor muscles, indicating that changes in capillary blood volume on CEU were functional in nature.

Skeletal muscle blood flow reserve was assessed during contractile exercise produced by electrostimulation of the adductor muscles. In control limbs, skeletal muscle blood flow reserve ranged from 3.0- to 3.5-fold and was not significantly different for different time intervals or different treatment groups. Skeletal muscle blood flow reserve in the ischemic limb was significantly reduced immediately after iliac artery ligation and, unlike resting

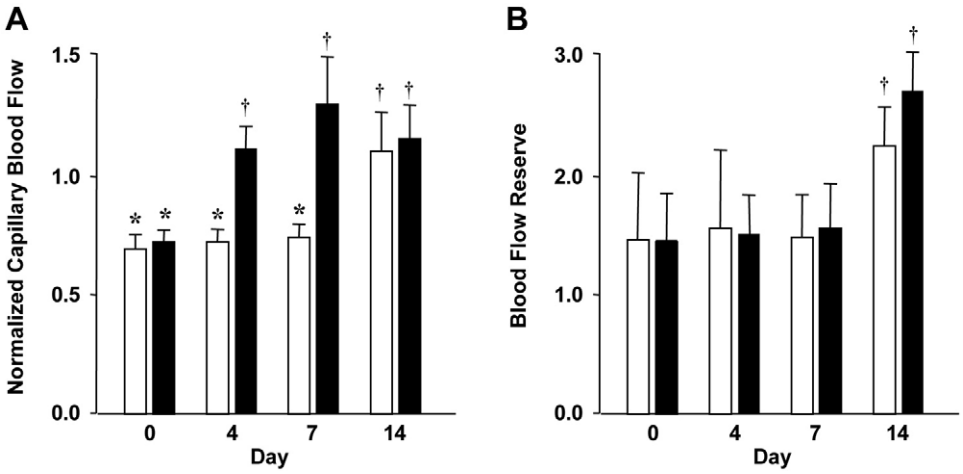


**Figure 2** (A) Mean (± standard error of the mean [SEM]) capillary blood flow relative to the contralateral control limb and (B) mean (± SEM) blood flow reserve in the ischemic limb for untreated (*white bars*) and FGF-2–treated (*black bars*) ischemic muscle. *$P < .05$ for ischemic versus control muscle data. †$P < .05$ versus corresponding day 0 data.

**Table** Mean change in relative capillary blood volume and velocity in ischemic muscle from immediate postocclusion values

| | Day 4 | Day 7 | Day 14 |
|---|---|---|---|
| Ischemia | | | |
| Cap velocity (β) | −3% | 7% | 33%* |
| Cap volume (A value) | 6% | 3% | 15%* |
| Ischemia + FGF-2 | | | |
| Cap velocity (β) | 33%* | 53%* | 42%* |
| Cap volume (A value) | 13% | 24%* | 15%* |

*FGF-2*, Fibroblast growth factor-2; *Cap*, capillary.
*$P < .05$ for change relative to values immediately postocclusion.

blood flow data, did not improve until day 14 in both treatment groups (Figure 2B).

### Remodeling of the Noncapillary Microcirculation

NCM blood volume was acutely reduced by iliac artery ligation and increased more rapidly and to a greater extent in FGF-2–treated limbs (Figure 3). Only in FGF-2–treated limbs did NCM blood volume exceed that of the normal limb at any time point. Immunohistology was used to determine the anatomic basis for the changes in NCM blood volume detected by CEU. On histology, both microvascular density and the fractional area of the NCM increased in the two groups in a similar pattern as CEU (Figure 4). The increase in NCM area was attributable to both a proliferation in the number of small (20-40 μm) vessels within muscle bundles and enlargement of larger transverse arterioles that bridged major muscle bundles.

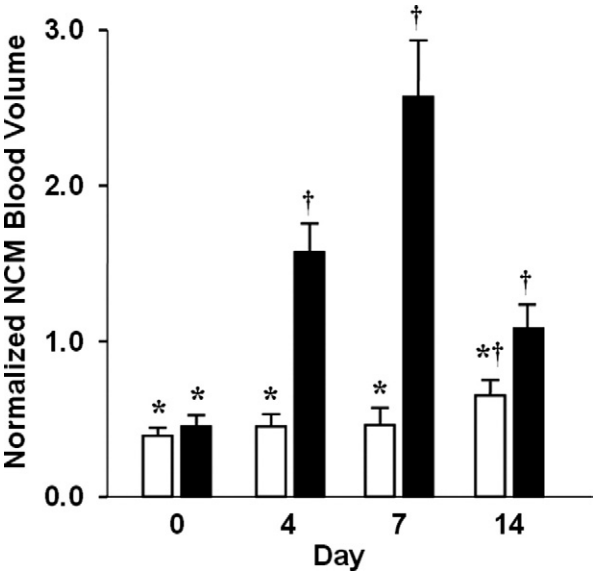


**Figure 3** Mean (± SEM) NCM blood volume relative to the contralateral control limb for untreated (*white bars*) and FGF-2–treated (*black bars*) ischemic muscle. *$P < .05$ for ischemic versus control muscle data. †$P < .05$ compared with corresponding day 0 data. *NCM*, Noncapillary microvessels.

### Blood Flow in Large Collateral Circuits

In nonischemic control limbs, signal enhancement on MIP imaging in the parasagittal plane was dominated by large intramuscular vessels down to the second branch order from the major penetrating vessel and a velocity of 20 mm/s or more. However,

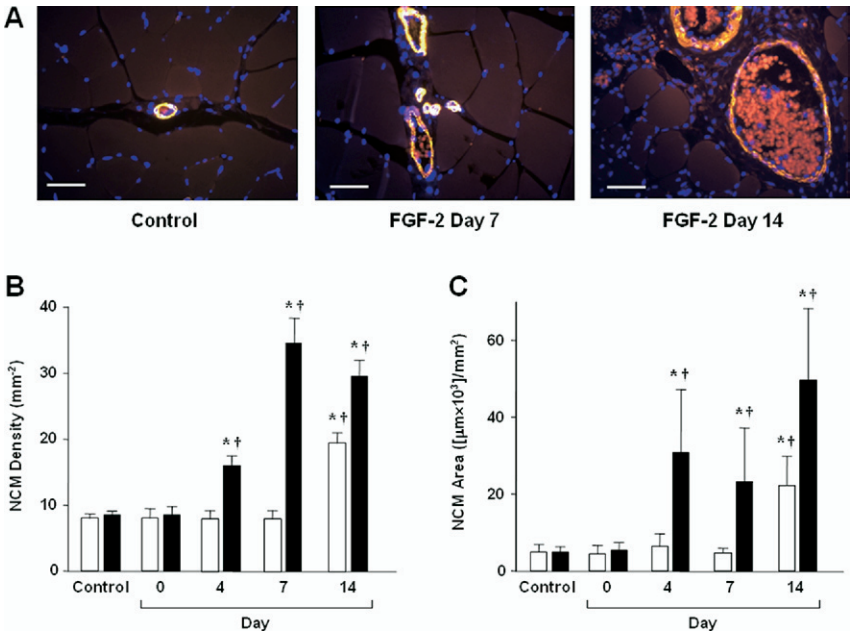


**Figure 4** Immunohistologic assessment of changes in the noncapillary microcirculation. (A) Merged images of DAPI and smooth muscle α-actin (ALEXA-555; Molecular Probes) staining in a control nonischemic muscle (at day 7) and in FGF-2–treated ischemic muscle at days 7 and 14. The images from the ischemic limb illustrate proliferation of small intramuscular NCM and enlargement of transverse interfiber vessels. Scale bar = 50 μm. (B) Mean (± SEM) NCM density and (C) NCM two-dimensional area as a ratio to the total area in untreated (*white bars*) and FGF-2–treated (*black bars*) ischemic muscle. *$P < .05$ versus control data. †$P < .05$ versus day 0. *FGF-2*, Fibroblast growth factor-2; *NCM*, noncapillary microvessels.

more distal vessels were detected in the terminal 500 milliseconds of the 2-second acquisition period with velocities as low as 10 mm/s and a third to fourth branch order consistent with the level of medium-sized arterioles (50-100 μm).[7,12,13] Immediately after iliac artery ligation, active flow was present in only a few large conduit arteries and veins with a paucity of distal microvascular enhancement, resulting in a much lower MIP video intensity at the completion of the acquisition period (Figure 5A). The number of vessels with active flow in the ischemic limb increased in a time-dependent fashion and was associated with gradual restoration of contrast propagation to the distal vessels (Figure 5A and video supplement). The normalized background-subtracted acoustic intensity on MIP imaging, an index of the number of actively perfused vessels, increased earlier for FGF-2–treated versus non-treated ischemic muscle, although peak recovery did not occur until day 14 for both groups (Figure 5B). Fractal dimension analysis demonstrated that ordered distribution of flow also increased more rapidly in FGF-2–treated ischemic limbs (Figure 5C). These data indicate a gradual improvement in the spatial apportioning of functional vessels ranging in size from medium microvessels to intramuscular arteries and veins.

## DISCUSSION

In this study, novel CEU imaging methods were applied in a model of peripheral vascular disease to characterize the continuum of vascular adaptations that occur in response to ischemia and growth factor therapy. Our findings indicate that the temporal course of recovery of nutrient blood flow in ischemic limbs parallels a functional expansion of the noncapillary microvasculature. The distal microcirculation also appears to be a major site of action for FGF-2. Larger collateral networks evaluated by MIP imaging were less affected by FGF-2, and our data suggest that substantial recovery in perfusion can occur before completion of remodeling of these vessels.

### CEU Imaging of Angiogenesis

One novel methodologic feature of this study was the modification of a perfusion imaging protocol that

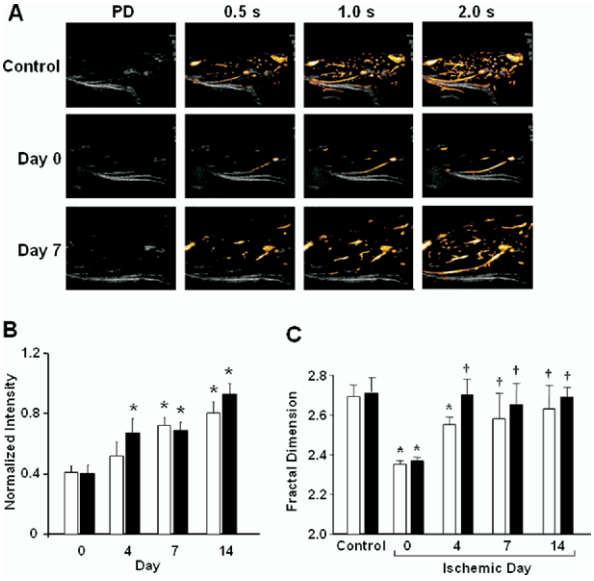


**Figure 5** MIP imaging of actively perfused large intramuscular vessels. (A) Parasagittal images of the proximal hind limb from control nonischemic and ischemic limbs (without FGF-2) immediately after arterial ligation (day 0) and at day 7. Frames displayed were obtained immediately post-destruction and at subsequent time intervals. (B) Mean (± SEM) background-subtracted intensity on the final MIP frame, normalized to the control limb, for untreated (*white bars*) and FGF-2–treated (*black bars*) ischemic muscle. *$P < .05$ versus day 0. (C) Mean (± standard deviation) fractal dimension of contrast enhancement at the end of the 2-second MIP acquisition for untreated ischemic muscle. Data were similar and grouped for the control leg at different time intervals and for the ischemic limb immediately after ligation (day 0). *$P < .05$ versus control leg. †$P < .05$ versus day 0. *PD*, Postdestruction.

enabled us to separately analyze capillary and NCM compartments in skeletal muscle. Assessment of blood flow with CEU has relied on measuring the product of microvascular blood volume and velocity.[6,8] When imaging the heart, these parameters reflect primarily capillary physiology because the majority of the intramyocardial blood volume resides in the capillary compartment.[14] Evaluation of coronary collateral flow in past studies has relied on the measurement of capillary perfusion, the end result of vascular remodeling.[4,5] In limb skeletal muscle, a greater proportion of the intramuscular blood volume at rest resides in larger vessels. To evaluate the functional impact of vascular remodeling, an image processing algorithm was used that eliminates signal from noncapillary vessels. Key components of this method are (1) the nonlinear relation that exists between vessel diameter and blood velocity[7] and (2) the alignment of the imaging plane perpendicular to the axial direction of most medium to large vessels. This algorithm has been applied recently to measure skeletal muscle capillary recruitment and shunting to nutritive vascular pathways in response to insulin and exercise and has been validated against assays for capillary xanthine oxidase availability.[8,9] Its application in this study to measure changes in nutritive capillary perfusion that occur from vascular remodeling represents a significant advance because other imaging techniques commonly used for this purpose, such as laser Doppler flow imaging, can neither isolate capillary flow nor provide information from a single tissue of interest.

The image processing algorithm also provided a means to measure NCM blood volume. This parameter is an index of the functional status of small to medium microvessels with flow velocities greater than 2 mm/s, thereby representing vessels just larger than skeletal muscle capillaries under resting conditions.[7,15,16] This method relies on selective detection of signal from vessels with a certain blood velocity range because true resolution of these vessels is not possible with the selected frequency bandwidth. Changes in NCM by CEU correlated temporally with arteriolar proliferation and enlargement on immunohistology. The relative magnitudes of change were not identical probably because of the functional rather than anatomic information provided by in vivo ultrasound imaging. The application of MIP imaging to evaluate the functional status of larger intramuscular vessels represents an important advance for assessing the morphometry of vessels that have traditionally been below the resolution of conventional ultrasound imaging.

### Large and Small Vessel Remodeling

In our model of hind limb ischemia, recovery of resting perfusion occurred 14 days after ligation in untreated animals, whereas recovery was much more rapid with FGF-2 treatment. These findings were similar to those in which collateral-dependent flow circuits were evaluated by radiolabeled microsphere injection or pressure-flow relations, albeit with different animal models and methods for FGF-2 delivery.[17,18] Recovery of perfusion was manifest primarily by an improvement in capillary blood velocity, suggesting a pressure correction at the precapillary level.[19] We do not believe that the vasodilatory effects of FGF were the primary reason for resting flow changes because (1) exogenous FGF-2 should be absent by several days,[10] (2) there was anatomic evidence of remodeling on immunohistochemistry, and (3) vasodilation alone would not be expected to produce significant changes in capillary blood volume. Although FGF therapy increased resting blood flow faster than in untreated animals, a significant improvement in blood flow reserve was not seen until day 14 in both groups of animals. At this time point, flow reserve tended to

be greater in the FGF-2–treated animals but still did not reach that of the normal control limb.

Previous studies demonstrated that proximal arterial obstruction is associated with time-dependent ultrastructural remodeling of preexistent vascular connections and improvement in large collateral arterial conductance.[20-22] These events were detected by the progressive increase in the number of actively perfused large intramuscular vessels on MIP imaging. However, our data also indicate that vascular adaptations in small NCM are critical for recovery of resting blood flow. Capillary flow did not improve until there was functional expansion of the distal NCM secondary to arteriolar enlargement and proliferation, which was also probably detected by distal enhancement (third to fourth order vessels) on MIP imaging. These findings suggest that large collateral circuits are most effective at restoring tissue perfusion only once there is remodeling of more distal small to medium arterioles, which reduces distal runoff resistance in the face of persistently low distal perfusion pressures. Remodeling of transverse arterioles would also improve collateral flow distribution between muscle groups, which was likely responsible for the increases in fractal distribution of flow. In other words, we believe that as collateral development occurs, there is coexistent remodeling in the more distal microcirculation that acts to reduce total network resistance and to distribute flow to the entire vascular network from collateral conduit entry points. The relative contribution of the adaptations that occur at each vascular level is still, however, not entirely known. The reason why there is a 2-week delay in small vessel remodeling in untreated limbs is not known, although this may represent a second adaptive phase that relies on upstream remodeling to produce sufficient shear stimulus to the distal microcirculation. It would also explain the progressive increases in total vascular conductance that have been detected late (>7 days) after large collaterals have formed.[21,22]

FGF-2 has been shown to augment flow through medium to large collateral vessels.[17,18] According to MIP data in this study, FGF-2 resulted in more rapid development of large collateral circuits than in untreated ischemic limbs, although these differences were small. Our data suggest that improved tissue perfusion at rest with FGF-2 was, at least in part, secondary to a marked functional expansion of the NCM (small arterioles and venules) and more ordered distribution of flow within muscle. Earlier remodeling of small to medium arterioles with FGF-2 may have been secondary to a direct effect that negated the need for shear stimulus and/or earlier shear stimulus from more effective upstream large vessel remodeling. It must be noted, however, that the late recovery of flow reserve and the fact that flow reserve still did not equal that in the normal control limb on day 14 indicate that abnormalities in total vascular resistance are still present despite recovery of resting blood flow.

## LIMITATIONS

An important limitation of this study is that the method for vascular segmentation was based on blood velocity gradients. It was unlikely that segmental flow velocity patterns remained constant. Reduction in flow velocity from arterial occlusion would be expected to artifactually shift a portion of the NCM signal to the capillary domain. We believe, however, that this underestimation was relatively small given that microvascular velocity at its lowest was only reduced by 20% compared with control. Moreover, in FGF-2–treated limbs, functional NCM actually exceeded that of the normal limb. Similarly, it must be noted that a small fraction of the capillary signal will be misappropriated to the NCM (illustrated in Figure 1 by the portion of the capillary signal replenished in <2 seconds). On the basis of the rate constants (β values) in this study, we estimate that capillary blood volume underestimation was less than 20% for all stages. Other limitations include the lack of dose response for FGF-2 and the selection of only proximal hind limb muscle for analysis. The relative degree of flow reduction and recovery of flow and reserve would likely have been greater if more distal muscle beds were studied.[23] We chose to study proximal muscle so that tissue volume was adequate for these new forms of small animal contrast ultrasound imaging, particularly for MIP imaging. An important limitation of the study is that no gold standard of blood flow, such as radiolabeled microsphere analysis, was used in this study. The technique has, however, been validated previously against microsphere techniques and pressure gradient measurements in models of coronary and peripheral vascular disease.[6,24,25]

## SUMMARY

This study provided several new concepts relating to limb neovascularization. From a methodologic standpoint, we demonstrated that noninvasive imaging with CEU may be an effective tool for studying the complex series of vascular events that occur in response to ischemia or growth factor therapy. Our data also suggest that recovery of capillary perfusion is at least partly dependent on remodeling at the level of small to medium microvessels that participate in further lowering of network resistance and flow distribution between muscle units, which can be modulated by growth factor therapy.

## REFERENCES

1. Helisch A, Schaper W. Arteriogenesis: the development and growth of collateral arteries. Microcirculation 2003;10:83-97.
2. Simons M. Angiogenesis: where do we stand now? Circulation 2005;111:1556-66.
3. Gössl M, Zamir M, Ritman EL. Vasa vasorum growth in the coronary arteries of newborn pigs. Anat Embryol 2004;208: 351.
4. Firoozan S, Wei K, Linka A, Skyba D, Goodman NC, Kaul S. A canine model of chronic ischemic cardiomyopathy: characterization of regional flow-function relations. Am J Physiol Heart Circ Phsyiol 1999;276:H446-55.
5. Villanueva FS, Abraham JA, Schreiner GF, et al. Myocardial contrast echocardiography can be used to assess the microvascular response to vascular endothelial growth factor-121. Circulation 2002;105:759-65.
6. Wei K, Jayaweera AR, Firoozan S, Linka A, Skyba DM, Kaul S. Quantification of myocardial blood flow with ultrasound-induced destruction of microbubbles administered as a constant venous infusion. Circulation 1998;97:473-83.
7. House SD, Lipowsky HH. Microvascular hematocrit and red cell flux in rat cremaster muscle. Am J Physiol Heart Circ Physiol 1987;252:H211-22.
8. Dawson D, Vincent MA, Clarke A, et al. Assessment of capillary recruitment in skeletal muscle using contrast-enhanced ultrasound. Am J Physiol Endocrinol Metab 2002; 282:E714-20.
9. Vincent MA, Clerk LH, Lindner JR, et al. Microvascular recruitment is an early insulin effect that regulates skeletal muscle glucose uptake in vivo. Diabetes 2004;53:1418-23.
10. Edelman ER, Mathiowitz E, Langer R, et al. Controlled and modulated release of basic fibroblast growth factor. Biomaterials 1991;12:619-26.
11. Dubuc B, Roques-Carmes C, Tricot C, Zucker SW. The variation method: a technique to estimate the fractal dimension of surfaces. Proc SPIE Int Soc Opt Eng 1987;845:241-8.
12. Marshall JM. The influence of the sympathetic nervous system on individual vessels of the microcirculation of skeletal muscle of the rat. J Physiol 1982;332:169-86.
13. Schmid-Schönbein GW, Firestone G, Zweifach BW. Network anatomy of arteries feeding the spinotrapezius muscle in normotensive and hypertensive rats. Blood Vessels 1986; 23:34-49.
14. Kassab GS, Lin DH, Fung YB. Topology and dimensions of pig coronary capillary network. Am J Physiol Heart 1994;267: H319-25.
15. Renkin EM. Control of microcirculation and blood-tissue exchange. In: Renkin EM, Michel CC, eds. Handbook of Physiology, Volume IV. Bethesda, MD: American Physiology Society; 1984:627-86.
16. Honig CR, Odoroff CL, Frierson JL. Capillary recruitment in exercise: rate, extent, uniformity, and relation to blood flow. Am J Physiol Heart Circ Physiol 1980;238:H21-42.
17. Kondoh K, Koyama H, Miyata T, Takato T, Hamada H, Shigematsu H. Conduction performance of collateral vessels induced by vascular endothelial growth factor or basic fibroblast growth factor. Cardiovasc Res 2003;61:132-42.
18. Yang HT, Deschenes MR, Ogilvie RW, Terjung RL. Basic fibroblast growth factor increases collateral blood flow in rats with femoral arterial ligation. Circ Res 1996;79:62-9.
19. Jayaweera AR, Wei K, Bin JP, Coggins M, Goodman C, Kaul S. Role of capillaries in determining coronary blood flow reserve. Am J Physiol Heart Circ Physiol 1999;277:H2363-72.
20. Ito WD, Arras M, Scholz D, Winkler B, Htun P, Schaper W. Angiogenesis but not collateral growth is associated with ischemia after femoral artery occlusion. Am J Physiol Heart Circ Physiol 1997;273:H1255-65.
21. Hoefer IE, van Royen N, Buschmann IR, et al. Time course of arteriogenesis following femoral artery occlusion in the rabbit. Cardiovasc Res 2001;49:609-17.
22. Herzog S, Sager H, Khmelevski E, Deylig A, Ito WD. Collateral arteries grow from preexisting anastamoses in the rat hindlimb. Am J Physiol Heart Circ Physiol 2002;283: H2012-20.
23. Lloyd PG, Yang HT, Terjung RL. Arteriogenesis and angiogenesis in rat ischemic hindlimb: role of nitric oxide. Am J Physiol Heart Circ Physiol 2001;281:H2528-38.
24. Bragadeesh T, Sari I, Pascotto M, Micari A, Kaul S, Lindner JR. Detection of peripheral vascular stenosis by assessing skeletal muscle flow reserve. J Am Coll Cardiol 2005;45: 780-5.
25. Wei K, Jayaweera AR, Firoozan S, Linka A, Skyba DM, Kaul S. Basis for detection of stenosis using venous administration of microbubbles during myocardial contrast echocardiography: bolus or continuous infusion? J Am Coll Cardiol 1998;32: 252-60.

## APPENDIX

The variation method has been adopted in this article to compute the fractal dimension (FD) of images. An image $Z(x, y)$ of size $M \times N$ can be considered as a surface of size $M \times N$, with a height of $Z(x_o, y_o)$ at position $(x_o, y_o)$. If a surface $Z$ is a fractal, there exists at least one part of the interval [0, 1] in which $Z$ is nowhere or almost nowhere differentiable. If $P(x, y, x', y')$ is the slope of the line passing through points $(x, y, Z(x, y))$ and $(x', y', Z(x', y'))$, then $|P(x, y, x', y')|$ goes to infinity as the point $(x', y')$ converges toward $(x, y)$. The FD is defined as the rate in which $|P(x, y, x', y')|$ goes to infinity. The variation of $Z$ can be defined as:

$$V_\varepsilon(x, y) = \max_{dist((x, y), (s, t)) \le \varepsilon} Z(s, t) - \min_{dist((x, y), (s, t)) \le \varepsilon} Z(s, t) \qquad (1)$$

where $dist((x, y), (s, t)) = \max(|x-s|, |y-t|)$ and $\varepsilon > 0$ is the scale parameter. The integral of $V_\varepsilon(x, y)$ converges to zero as $\varepsilon$ converges to 0. The rate of growth of this integral is directly related to the FD of $Z$. The FD of the surface $Z$ is then defined as:

$$FD_z = \lim_{\varepsilon \to 0} \frac{\log \int_0^1 \int_0^1 \frac{V_\varepsilon(x, y)}{\varepsilon^3} dxdy}{\log \frac{1}{\varepsilon}} \qquad (2)$$

The slope of the log-log plot of the line that is defined by $\log \iint [V_\varepsilon(x, y)/\varepsilon^3]\, dxdy$ and $\log(1/\varepsilon)$ provides the FD of the surface. The computation of the FD of a surface involves substitution of the integrals with summations. In the case where localized FD extraction is required, the FD may be computed

locally in image regions of size $R \times R$ centered at each and every image pixel to create an FD map of size $M \times N$. Therefore, the FD space is mapped one-to-one to the pixels of the image.

The algorithm for calculating the FD of an image is as follows: The variation $V_\varepsilon$ defined as difference between the maximum and the minimum grayscale values is computed in a small window of size $T \times T$, where $T = 2\varepsilon + 1$. This window is centered at the image pixel with coordinates $(x, y)$. This computation is repeated for all pixels $(x, y)$ of the image, for different values of ε. Then, $V_\varepsilon(x, y)$ is the ε - th variation located at $(x, y)$. If we define $E_\varepsilon$ as the average variation $V_\varepsilon(x, y)$ in the image, the FD is calculated as the slope of the line that best fits the points $(\log(R/\varepsilon), \log\{(R/\varepsilon)^3 E_\varepsilon\})$ where $\varepsilon = 1, 2, 3, \ldots, \varepsilon_{max}$. The line that best fits these points can be found using linear regression.

## SUPPLEMENTARY DATA

Supplementary data associated with this article can be found, in the online version, at 10.1016/j.echo.2007.02.016.